

Ecological modeling based on benthic foraminifera from Tupilipalem coast, southeast coast of India: Implications for ecological trajectory

Sreenivasulu Ganugapenta (✉ seenu9441@gmail.com)

Yogi Vemana University <https://orcid.org/0000-0002-2781-0463>

Jayaraju Nadimikeri

Yogi Vemana University

Lakshmana Ballari

Yogi Vemana University

Prakash Thirumali Nagesh Rao

National Centre for Earth Science Studies

Varghese Itty Tiju

National Centre for Earth Science Studies

Nallapa Reddy Addula

Oil and Natural Gas Corporation Ltd

Research Article

Keywords: Benthic foraminifera, Bio-proxy, Heavy Metal Pollution, Coastal Morphodynamics, Dugarajapatnam Port, Southeast Coast of India.

Posted Date: April 1st, 2021

DOI: <https://doi.org/10.21203/rs.3.rs-382408/v1>

License: © ⓘ This work is licensed under a Creative Commons Attribution 4.0 International License.

[Read Full License](#)

Ecological modeling based on benthic foraminifera from Tupilipalem coast, southeast coast of India: Implications for ecological trajectory

Sreenivasulu Ganugapenta^{1*}, Jayaraju Nadimikeri¹, Lakshmana Ballari¹, Prakash Thirumali Nagesh Rao², Varghese Itty Tiju², Nallapa Reddy Addula³, Nagendra Raghavendramurthy⁴, Leela Sheela Nair²

¹ Department of Geology, Yogi Vemana University, Kadapa- 516005, Andhra Pradesh, India

² Marine Geoscience Group (MGG), ESSO- National Centre for Earth Science Studies (NCESS), Thiruvananthapuram- 695011, India

³ Former Chief Geologist, Oil and Natural Gas Corporation (ONGC), Chennai-600076, India.

⁴ Department of Geology, Anna University, Chennai- 600025, India.

**Corresponding author : seenu9441@gmail.com*

Abstract

Landsat 8 OLI/TIRS data of Tupilipalem coast demonstrates the periodic closure of lagoon mouth over a brief period affecting the ecological setting and the faunal diversity and distribution. The coastal ecosystem includes a significant metal pollutant due to anthropogenic activities. This study documents forty-nine numbers of benthic foraminiferal species and establishes its relationship with heavy metal concentrations (Fe, Mn, Cr, Cu, Ni, Pb, Zn and Cd). The factor loading matrix generated using factor analysis grades the positive and negative correlations among the heavy metals species. The results of geoaccumulation index, enrichment factor, and pollution load index, construes the seasonal differences in metal

concentrations and prevalence of higher concentrations of metals in the sediments. Besides, this paper discusses the impact of coastal morphology on heavy metal concentrations coupled with ecology and distribution of benthic foraminifera.

Keywords: Benthic foraminifera, Bio-proxy, Heavy Metal Pollution, Coastal Morphodynamics, Dugarajapatnam Port, Southeast Coast of India.

1. Introduction

The application of benthic foraminifera is a potential tool for environmental monitoring of polluted scenarios (Martins et al., 2016; Sreenivasulu et al., 2017b; Martins et al., 2019). The interactions between organisms and their habitats serve as proxies to comprehend the management of marine populations (Roff et al., 2003; Adarsh & Rajeshwara Rao, 2012). Benthic foraminifera, its abundance and diverse protists in ecosystems (Sreenivasulu, et al., 2017a), are applied to investigate the environmental status of region for over a century (Jayaraju et al., 2010). The foraminifera are successful inhabitants from deep ocean to brackish water lagoons, estuaries and, lakes (Solai et al., 2013; Sreenivasulu et al., 2017b; Suresh Gandhi and Jisha, 2017). The changes in benthic faunal abundance, species diversity, environment quality, sensitivity to a specific environment and variation in morphology of tests provide an evidence for change in ecological parameters (Boltovskoy et al., 1991; Holzhauser et al., 2020; Bouchet et al., 2012; Bouchet et al., 2020).

The coastal ecosystem is under stress and cryptic degradation from pervasive exposure to various anthropogenic activities (Crain et al., 2009; Cochard, 2017). Over the last few decades, anthropogenic influx of heavy metals into the aquatic ecosystem has increased to alarming magnitude (Ansari et al., 2003; Gheorghe et al., 2017; Pandey & Singh, 2017; Cardoso et al., 2019; Reid et al., 2019). As a result, ecosystems have chronic inputs of metals thus contaminated sediments heavily (Qian et al., 2015; Soliman et al., 2015; Liu et al., 2020;

Tian et al., 2020). The consequence of the non-degradable state of heavy metals, causes for bioaccumulation in the food chains (Singh et al., 2011). This work aims to propose a model to understand the impact of coastal morphological changes on the lagoon mouth by affecting the concentrations of heavy metal in the sediments and taxonomic composition, quantitative distribution and test morphologies of benthic foraminifera. The ecological trajectory results are a reference of baseline datasets for further comparison of changes in coastal morphodynamics, sediment biogeochemical properties and function as benchmark.

2. Study area

Tupilipalem is likely to be developed as a major sea port named as Dugarajapatnam Port by the Government of India (Fig. 1). The study area is geographically located on southeastern part of India, lying between latitude $14^{\circ}0'10'' - 14^{\circ}02'30''$ N and longitude $80^{\circ}08'20'' - 80^{\circ}19'00''$ E. Tupilipalem is over 120 km away from Pulicat Lake and the satellite launching center (SHAR) at Sriharikota. The Buckingham Canal is part of the lagoon on its western side. This lagoon (mouth) connects to the open Bay forms the study area. The subtropical climate prevails over the study area with an average annual rainfall of 1041 mm. The average minimum and maximum temperatures are 20°C and 39.6°C respectively. However, the currents are also affected by the tidal cycles, by the action of waves, the shore line geography and by the presence of different water masses, assuming predominantly a SW-NE direction (Sreenivasulu et al., 2017).

3. Methodology

3.1. Coastal morphology

To detect the coastal morphodynamics, multi temporal satellite images of Landsat 8 OLI/TIRS data during monsoon and Pre-monsoon were downloaded from USGS, Earth Explorer (Sreenivasulu et al., 2017). Then each image was cropped using area of interest

cropping method. The cropped images were geometrically corrected by using the auto-sync tool in ERDAS Imagine 9.1 software by applying the UTM- WGS 84 projection and coordinate system (Chenthamilselvan et al., 2014). Wind components with a resolution of 0.125°x 0.125° were obtained from the European Centre Medium-range Weather Forecast (ECMWF). Wind speed and direction maps were plotted using Coastline+ and MATLAB (Satar et al., 2020).

3.2. Sample collection

Twenty six sediment samples were collected from 13 sampling stations during two seasons (monsoon and Pre-monsoon) by using a grab sampler. The position of the sampling stations was located using a Global Positioning System (GPS).

3.3. Geochemical Analysis

About 1g of dried sediment samples were digested (at 110°C for 90 min) with 14 ml of aqua-regia solution (HNO₃:HCl). After cooling, 14 ml of aqua-regia was added and heated again at 110°C for 30 minutes. The digested samples were filtered through 0.45 µm membrane and the concentrations of heavy metals (Fe, Mn, Cr, Cu, Ni, Pb, Zn and Cd) were measured by inductively coupled plasma-optical emission spectrometry (ICP-OES) (Trevizan & Nóbrega, 2007; He et al., 2017; Lai et al., 2018). To understand the existing environmental condition and the amount of heavy metal contamination with respect to the natural environment, other indices were applied like Geoaccumulation Index (I_{geo}), Enrichment Factor (EF) and Pollution Load Index (PLI) (Ahmed et al., 2016; Kowalska et al., 2018; Sreenivasulu et al., 2018; Shirani et al., 2020).

Geoaccumulation Index (I_{geo}) is calculated using the following equation:

$$I_{geo} = \log_2 \left(\frac{C_n}{1.5 B_n} \right)$$

Where C_n is the concentration of element 'n', B_n is the geochemical background value and 1.5 is a factor for potential variation in background data due to lithogenic effect.

The EF is calculated using the following equation

$$EF = \frac{M_x \times Fe_b}{M_b \times Fe_x}$$

Where M_x is sediment sample concentration of the heavy metal, Fe_x is the Fe concentration in the sediment, M_b and Fe_b are their concentrations in a suitable background or baseline reference material.

The Pollution Load Index (PLI) is calculated as:

$$PLI = \sqrt[n]{CF_1 \times CF_2 \times CF_3 \times \dots \times CF_n}$$

Where n is the number of metals and contamination factor CF is given by $CF = C_{metal} / C_{background}$, (C_{metal} is the corresponding metal concentration of the sample and $C_{background}$ metal concentration in the back ground)

3.4. Benthic foraminiferal analysis

For the benthic foraminiferal analysis, sediments were washed over a 0.625 mm mesh to obtain samples devoid of fine silt and clay. Then the residue was air dried and nearly 50 g of sample obtained by coning and quartering. All subsamples were examined under a Stereo Zoom Binocular Microscope and foraminifer tests from each sample were picked using a Windsor Newton Sable Hair brush ("000") and identified following the taxonomic classification of Brady (1884), Loeblich and Tappan (1987), Foraminifera and gallery-illustrated catalog (www.foraminifera.eu), World Modern Foraminifera Database (www.marinespecies.org/foraminifera/) and Paleontologia Electronica Webmaster 1998-2015. The quantitative foraminiferal data were used for computing various statistical

parameters including total individual abundance (N), species richness (d), species evenness (J), Shannon–Wiener diversity index (H), Ammonia- Elphidium Index (AEI) and FORAM Index (FI) in the assemblages.

Species richness (d) is calculated using the following formula

$$d = \frac{S}{\sqrt{N}}$$

Where S= The number of different species present in the sample, N= total number of individual species in the sample.

The Shannon-Wiener Diversity Index (H) is calculated using the following equation:

$$H = \sum_{i=1}^s -(P_i * \ln P_i)$$

Where H = the Shannon diversity index, P_i = fraction of the entire population made up of species i, s = numbers of species encountered and \sum = sum from species 1 to species S.

Species evenness (J) was calculated as

$$J = \frac{H}{H_{\max}}$$

Where H= Shannon- Wiener Diversity Index; H_{\max} = Maximum possible value of H.

The Ammonia-Elphidium Index (AEI) described by Sen Gupta et al., (1996) was calculated as

$$AEI = \frac{NA}{NA + NE} \times 100$$

Where NA= Total number of Ammonia/ sample, NE= Total number of Elphidium/ sample.

The FORAM Index (FI) was calculated using the following formula:

$$FI = (10 \times Ps) + (Po) + (2 \times Ph)$$

In which, FI = FORAM Index, $P_s = N_s / T$, with “Ns” the number of symbiont-bearing foraminifers, $P_o = N_o / T$, with "No" the number of opportunistic foraminifers and $P_h = N_h / T$, with “Nh” the number of other small, heterotrophic foraminifers, T= Total number of foraminifera.

3.5. Statistical analyses

Factor analysis (FA), which is the most common multivariate statistical method was used to reduce data and to extract a small number of latent factors for analyzing relationships among the observed variables by using XLSTAT 2018. Hierarchical cluster analysis (HCA) was used to estimate similarities in species composition among the samples. The data were logarithmically transformed to reduce the score and bias of higher values that may have otherwise masked the effect of lower values.

4. Results

4.1. Coastal Morphology

Coastal morpho-dynamics are the marine, physical, meteorological and biological activities that interact with the sediments to produce a particular coastal environmental setting (Short & Jackson, 2013). The waves and currents play a significant role in controlling sediment migration and deposition (Sreenivasulu et al., 2016). Wind-generated wave energy input into the littoral zone and, together with wave-generated currents are responsible for the alteration of coastal morphology. Remote sensing multi-temporal Landsat 8 OLI/TIRS images acquired on October 27, 2014 (Monsoon) and August 27, 2015 (Pre-monsoon) revealed that sandbar across the lagoon mouth is vastly dynamic. In Fig. 2, during monsoon the lagoon mouth closure was noticed and the image during pre-monsoon has two opening points at the northern and the southern parts of the lagoon. Out of two, one is the natural opening at northern side and another is a non-natural at southern side. The non-natural one is

opened by the villagers for their fishing boats passage during lagoonal mouth closure. Tupilipalem coast revealed that the rate of erosion and accretion reflects coastal dynamics and the loss or gain of sediments causes the formation of young beaches, berms, sand dunes and seacliffs depending on wave energy and littoral currents. Over the last five years (2011–2015), accretion is geological process over the erosion, which deposits the sediments in the lagoon mouth, causing the closure of the lagoon (Sreenivasulu et al., 2017 & 2018). In order to assess the factors influencing the morphological changes of lagoon mouth, wind speed and direction plots during the seven days prior to each satellite image were used. Thus, the wind strength is significant in large volume of sand transport. The prevailing northern wind causes an oblique wave approach to the shoreline, which generates a westward littoral transport (Fig. 3). Strong winds blowing above 2- 4 m/s are considered to be effective during monsoon and pre-monsoon. In conclusion, the strong onshore winds and large waves are the factors for the development of elevated water levels which allow the larger waves to transport sand to the shoreline and tend to deposit on the river mouth causing its closure. During pre-monsoon, the wind speed and direction has been changed (Fig. 4) in order to facilitate the open of lagoon mouth.

4.2. Geochemistry

4.2.1. Heavy Metals distribution

The variations of heavy metal concentrations (Fe, Mn, Cr, Cu, Ni, Pb, Zn and Cd) in different locations of Tupilipalem coast during monsoon and pre-monsoon are shown (Tables 1 and 2). The range and average concentrations (given in parenthesis) (ppm) were 942.1- 8138.14 (2507.99) for Fe, 16.16- 131.16 (52.07) for Mn, 4.27- 19.75 (9.94) for Cr, 2.02- 7.01 (3.29) for Cu, 2.98- 10.9 (5.68) for Ni, 3.69- 9.48 (5.53) for Pb, 11.3- 21.98 (14.85) for Zn and 0.49- 1.43 (0.85) for Cd in monsoon. In pre-monsoon, the range and average concentrations (given in parenthesis) (ppm) were 943.3- 8683.63 (3233.95) for Fe, 18.46-

169.24 (59.55) for Mn, 4.89- 22.32 (10.26) for Cr, 2.23- 6.96 (3.81) for Cu, 3.52- 10.45 (6.74) for Ni, 3.64- 7.53 (5.81) for Pb, 11.57- 24.75 (15.23) for Zn and 0.41- 1.09 (0.72) for Cd. These results exposed that greater variation was observed in Fe, Mn and Cr concentrations, whereas other elements showed a gradual trend between the various sampling sites. The decreasing trend of average contents of heavy metals was Fe > Mn > Zn > Cr > Ni > Pb > Cu > Cd.

The highest concentrations of Fe, Cr, Cu, Ni and Pb were observed at station TP-M in both the seasons which was located at the brackish environment where the Buckingham Canal and other aquacultural effluents were connected to the Bay of Bengal. This location is periodically closed and also predominantly covered with mangroves, showed the extent to which pollutants were being increased. It seemed that these parts of the study area were heavily affected by anthropogenic and natural sources of pollution. The highest concentration of Mn (131.16 ppm) and Zn (21.98 ppm) were observed at station TP-M in monsoon and station TP-5 [Mn (169.24 ppm) and Zn (24.75 ppm)] in pre-monsoon. The Cd showed the highest concentration (1.43 ppm) at station TP-7 in monsoon and station TP-8 (1.09 ppm) in pre-monsoon. The lowest concentrations of the studied heavy metals were reported at the stations TP-4 (Ni), TP-5 (Pb), TP-6 (Cr and Zn), TP-9 (Fe, Mn) and TP-10 (Cu and Pb) during the monsoon. In premonsoon, TP-2 (Cd), TP-3 (Pb), TP-7 (Fe, Cr and Cu), TP-8 (Mn and Ni) and TP-10 (Zn) were the stations which showed lowest concentrations of the heavy metals.

On a seasonal scale, Fe, Mn, Cr and Zn showed their highest values (8683.63, 169.24, 22.32 and 24.75 ppm) during the pre-monsoon where the lowest values (942.1, 16.16, 4.27 and 11.3 ppm) were exhibited during monsoon. Cu and Ni recorded the maximum (7.01 and 10.90 ppm) and the minimum (2.02 and 2.98 ppm) during the monsoon. Finally, Pb and Cd showed their highest concentration (9.48 and 1.43 ppm) during monsoon where the lowest

concentration (3.64 and 0.41 ppm) during the premonsoon. The highest concentration of Pb, Zn, Cd and Mn were reported from the lagoon environment during lagoon mouth closure period (monsoon).

4.2.2. Metal Enrichment Assessment

To understand the existing environmental condition and the amount of heavy metal contamination with respect to the natural environment, other approaches should also be applied. The anthropogenic contribution of the selected heavy metals in marine sediments can be estimated from the metal enrichment compare to the background levels. Various methods have been suggested for quantifying metal enrichment in surface sediments like Geoaccumulation Index (Igeo), Enrichment Factor (EF) and Pollution Load Index (PLI). Based on the Muller (1961) classification, Geoaccumulation Index (Igeo) includes 7 classes: $I_{geo} \leq 0$: practically unpolluted; $0 < I_{geo} < 1$: Unpolluted to moderately polluted; $1 < I_{geo} < 2$: Moderately polluted; $2 < I_{geo} < 3$: Moderately to strongly polluted; $3 < I_{geo} < 4$: Strongly polluted; $4 < I_{geo} < 5$: Strongly to extremely polluted; $5 < I_{geo}$: Extremely polluted (Varol, 2011). In this study, Igeo values are in the following ranges; Fe (25- 28), Mn (13- 17), Cr (8- 10), Cu (5- 7), Ni (7- 9), Pb (6- 7), Zn (10- 11) and Cd (-3- -2). The formula resulted from the analysis of large amounts of data revealed that Fe, Mn, Cr, Cu, Ni, Pb and Zn had a higher degree of contamination in both the seasons (monsoon and pre-monsoon) (Fig. 5).

The enrichment factor (EF) is a suitable measure of geochemical trends and is used for making comparisons among areas. In the present study, iron was used as a conservative tracer to differentiate natural from anthropogenic components. According to Sutherland, (2000), five contamination categories are reported on the basis of the enrichment factor, which are- $EF < 2$ deficiency to minimal enrichment, $EF = 2-5$ moderate enrichment, $EF = 5-20$ significant enrichment, $EF = 20-40$ very high enrichment, and $EF > 40$ extremely high

enrichment. Enrichment Factor (EF) during the monsoon, decreasing trend of the average contents enrichment factor was Cd > Pb > Zn > Cu > Cr > Ni > Mn > Fe. On applying the above contamination categories, Cd indexed extremely high enrichment in 70% of the stations (TP-6, TP-7, TP-8, TP-10, TP-9, TP-4) and 15% of the stations (TP-1, TP-2, TP-3, TP-5 and TP-M) showing very high enrichment. The Pb showed significant enrichment in 70% of the stations. Remaining 30% of the stations showed moderate enrichment. The Zn showed significant enrichment in 38% of the stations and moderate enrichment for 46% of the stations. Cu showed significant enrichment at the station TP-4 and 54% of the stations showing moderate enrichment. Cr and Mn showed significant enrichment at the stations TP-9 and TP-6 respectively. Cr and Ni showed moderate enrichment in 54% of the stations. The remaining heavy metal (Fe) showed a deficiency to minimal enrichment in all the stations. During premonsoon, decreasing trend of the average contents' enrichment factor was Cd > Pb > Zn > Cu > Cr > Ni > Mn > Fe. Cd indexed extremely high enrichment in 54% of the stations, 30% of the stations showing very high enrichment and remaining 16% of the stations showing significant enrichment. The Pb showed significant enrichment in 46% of the stations. Remaining 54% of the stations showed moderate enrichment. Zn showed significant enrichment at the station TP-7 and moderate enrichment for 70% of the stations. Cu showed moderate enrichment in 54% of the station. Cr showed moderate enrichment at the stations TP-2, TP-7 and TP-8 respectively. Ni showed moderate enrichment at the stations TP-1, TP-7 and TP-9. Moreover, the remaining heavy metals (Fe and Mn) showed deficiency to minimal enrichment in all the stations (Fig. 6).

The values of the Pollution Load Index (PLI) varied from 0.04 to 2.83 during monsoon and 0.05 to 2.33 during premonsoon respectively (Fig. 7). The PLI values of the Cd showed higher (>1) values during both the seasons (monsoon and premonsoon) due to the influence of direct external sources like agricultural runoff, industrial activities, and other

anthropogenic inputs. According to the GESAMP (1985), Cd comes from contaminated agricultural soils, mining waste, municipal sewage effluents and sludges and also derived from erosion of sulfide ores, phosphorites, hydrothermally mineralized rocks and black shale deposits. The analyzed metals like Fe, Mn, Cr, Cu, Ni, Pb and Zn recorded baseline levels (<1). The difference in indices results due to the difference in sensitivity of these indices towards the sediment pollutants (Praveena et al., 2007).

4.2.3. Factor Analysis

The selected heavy metal data were subjected to factor analysis. The analysis yielded three factors during monsoon, namely, Factor 1 (68.18 %), Factor 2 (16.49 %) and Factor 3 (6.56 %) (Figs. 8a and 8b). Factor 1 was represented by Fe (0.983) and Cu (0.936) (Table 3). Hence it may be termed as Fe- Cu assemblage. The assemblages were named according to their most dominant heavy metals. Factor 2 composed of Mn (0.729) and Cd (0.654) and named as Mn- Cd assemblage. In addition, Factor 3 was represented by Zn (0.398) and Cr (0.116) and it is called as Zn- Cr assemblage.

In pre- monsoon, factor loadings show that there are three distinguishable factors in the data: Factor 1 (70.62 %), Factor 2 (13.77 %) and Factor 3 (9.36 %). Factor 1 envelops two variables, Fe (0.965) and Cr (0.956). Hence it may be termed as Fe- Cr assemblage. Factor 2 is composed of two variables, Cd (0.963) and Zn (0.180). Therefore it is called as Cd- Zn assemblage. Factor 3 includes two variables, Pb (0.756) and Cu (0.231) and it is called as Pb- Cu assemblage. Finally, a cross plot of Factors 1&2 and Factors 1&3 gave distinct information about heavy metals distribution and set cluster of similar factor (Fe, Cu, Cd, Zn and Cr) during both the seasons (Figs 8c and 8d).

4.3. Ecology and Distribution of benthic foraminifera

Spatial distribution of total benthic foraminifer tests in terms of absolute numbers is given in (Tables 4 & 5). A total of 49 species, 19 genera and 3 suborders have been recognized. In monsoon, total population ranges from 5 to 271 with an average of 57 counts and in premonsoon, from 5 to 744 with an average of 84 counts per 100 grams dry sediment. *Ammonia dentata*, *A.beccarii*, *Quinqueloculina seminulum*, *Elpidium discoidale*, *E.crispum*, *Pararotalia nipponica*, and *Asterorotalia trispinosa* were the dominant species during the monsoon. And *Ammonia beccarii*, *A.parkinsoniana*, *Pararotalia nipponica*, *Ammonia dentata*, *A.tepida*, *Quinqueloculina seminulum* and *Q.venusta* were widely distributed during pre-monsoon. On seasonal scale, the higher number of individual species was increased from 271 (TP-3 beach environment) to 744 (TP-9 brackish environment) during monsoon to pre-monsoon respectively.

4.3.1. Diversity Indices

The values of Species richness (d) was ranges between 0.480 (TP-7) - 4.463 (TP-3) during monsoon and 0.961 (TP-6) - 4.235 (TP-9) during pre-monsoon. Species evenness (J) values ranged between 0.653 (TP-12) - 0.852 (TP-5) during monsoon and 0.745 (TP-7) - 0.960 (TP-5 and TP-M) during pre-monsoon. Shannon- Weiner Diversity index (H) was ranged between 0.05- 2.19 during monsoon and 0.9- 2.908 during pre-monsoon. The higher value of H was observed at station TP-3 and the lower value was observed at station TP-10. The H value from beach environment to brackish environment (lagoon) was significantly decreased during monsoon. The higher value of H was observed at the station TP-9 and the lower value of H was observed at the station TP-6. During pre-monsoon, both the lower and higher values were recorded from the lagoon (brackish environment). Finally, Diversity Indices values at the brackish environment (Lagoon) were significantly increased from monsoon (lagoon mouth closure) to pre- monsoon (lagoon mouth open) (Table 6 & Fig. 9).

4.3.2. Ecological Indices

The AEI was formerly established as an indicator of hypoxic conditions (Sreenivasulu et al., 2019). Studies have shown that the AEI has strong correlation with sediment hypoxia (Sen Gupta & Platon, 2006; Minhath et al., 2013). The AEI values ranged between 83.464- 100 during monsoon and 75- 100 during pre-monsoon. During monsoon, the higher value of AEI (100) was recorded at lagoon side (Stations TP-5, TP-6, TP-7, TP-8, TP-9, TP-10, TP-11 and TP-M) indicating greater hypoxic conditions (Fig. 10). The lower value of AEI (83.464) was observed at station TP-4 which is located at the beach environment indicating a lower influence of hypoxia at this site. During pre-monsoon, the higher value of AEI (100) was recorded at stations TP-5, TP-11, TP-12 and TP-M. the lower value (75) was observed at stations TP-3 and TP-8. The stations which show the higher value of AEI (100) were slightly decreased from monsoon to pre-monsoon. The FI values showed the lower ranged between 1-1.833 during monsoon and 1-1.454 during pre-monsoon (Fig. 10). FI values in both the seasons (Monsoon and pre-monsoon) were showing less than 2. According to Carnahan et al., (2009), $FI < 2$ indicates environmental conditions that support substantial populations of stress tolerant taxa such as *Ammonia spp.*

4.3.3. Deformed tests as indicators of polluted environments

Mode of test deformation depends on the degree of pollution and type of pollutants. Forms having corrosion, cavity development, broken peripheries and reduction in the overall growth are associated with high trace metal levels (Pati & Patra, 2012). Here are some of the abnormalities noted in the study area (Plates 1 & 2) i.e. corrosion, cavity development, broken peripheries and reduction in the overall growth. These abnormalities on the test morphology were taken as proxies of pollution signatures on the bio indicators in the present study caused by metal pollutants such as Cd, Zn, Cr, Cu, Fe, etc., released by external sources like agricultural runoff, industrial activities and other anthropogenic inputs.

5. Discussion

Cluster analysis divided the study area into three biotopes in both the seasons. Each biotope is characterized by a distinct foraminiferal assemblage related to ecological settings.

During monsoon, three biotopes were formed by the cluster analysis (Fig. 11). Biotope-I comprises only one station (TP-6). The higher value of Mn (11.029 ppm), Zn (11.3 ppm) and Cd (1.15 ppm) were recorded. In the enrichment factor analysis, Cd indexed extremely high enrichment. The lowest individual number of foraminifera species were reported where the *Ammina dentate* (1 species) and *Quinqueloculina seminulam* (5 species) are the only species found in this location. Diversity indices show the lower values with the foraminiferal data. The AEI showed the value '100' indicating greater hypoxic condition. Biotope-II includes stations TP-8, TP-M, TP-7, TP-9, TP-5, TP-10 and TP-11. In this biotope, all the stations showed the moderate number of foraminiferal species where *Ammonia beccarii* and *A. dentate* were the common species and all these stations were located in the lagoon side. All the lower values of diversity indices were reported from this biotope. AEI values (100) of all the stations of this biotope indicates greater hypoxic conditions and FI value (<2) indicates the stress conditions that support stress tolerant taxa. The highest values of all the studied heavy metals were reported from this biotope. Cd showed extremely high enrichment in all the stations. Biotope- III comprises of stations TP-12, TP-2, TP-4, TP-3 and TP-1. Except TP-12, remaining all the stations from beach environment and station TP-12 at the lagoon mouth from the lagoon side. Moderate to low values of heavy metal concentrations were reported from this biotope. The highest values of distribution and diversity indices were reported from these locations. *Ammonia dentate*, *A. beccarii*, *Quinquiloculina seminulam*, *Elphidium discoidale*, *E. crispum* and *Pararotalia nipponica* were the most dominant species in this biotope. The ecological indices of AEI and FI values were <100 and <2 respectively. AEI values indicates the lower influence of hypoxia

and FI values indicate that the environmental condition of the biotope supports substantial populations of stress tolerant taxa.

In pre-monsoon, the cluster analysis performed three clusters i.e Biotope-I, Biotope-II and Biotope-III (Fig. 12). Biotope-I comprised only one station i.e., TP-9 where the highest value of total individual foraminiferal species were reported. *Ammonia beccarii*, *A. parkinsoniana*, *A. tepida*, *Pararotalia nipponica*, *Milionilinella subrotunda* and *Nonion grateloupi* were the most dominant species in the biotope. The station TP-9 is located in the brackish environment (within the lagoon). Higher values of species richness (d), evenness (J) and diversity (H) were reported from this location. The AEI and FI values were 83.798 and 1.275 respectively and indicate that the lower influence of hypoxia and environmental stress condition. Biotope-II comprised stations TP-7, TP-4, TP-1, TP-2 and TP-3 where the heavy metal concentrations were moderately enriched. All the stations in this biotope were located in the beach environment except TP-7. Diversity indices showed moderate to higher values of species richness, evenness and diversity. An AEI values were less than 100 except station TP-1 indicates the moderate influence of hypoxia and <2 of FI indicates environmental conditions that support the survival of stress tolerant species. Species such as *Ammonia beccarii*, *A. dentate*, *Quinquiloculina seminulam* and *Q. stelligera* were the dominant. Biotope-III includes the stations TP-6, TP-8, TP-12, TP-10, TP-11, TP-5 and TP-M. These stations were located in the brackish environment (lagoon). Very meager population of stress tolerant species of foraminiferal were reported. *Ammonia* sp., *Quinquiloculina* sp., and *Spiroloculina* sp., are the most dominant species in this biotope. Lower values of diversity indices were recorded from these locations whereas the AEI indicated the greater influence of hypoxia from the stations.

On seasonal scale, lot of changes are observed during monsoon to pre-monsoon in the coastal morphology and lagoon mouth dynamics in particular. Consequently, the lagoon

mouth dynamic activity affecting the distribution of heavy metal concentrations, taxonomic composition and quantitative distributions in foraminiferal assemblages. The sampling stations from the brackish environment (TP-5, TP-6, TP-7, TP-8, TP-9, TP-10, TP-11, TP-12 and TP-M) during lagoon mouth closure (monsoon) showed highest concentrations of studied heavy metals and extremely high enrichment of Cd. The values due to the influence of direct external sources like agricultural runoff, industrial activities, and other anthropogenic inputs. Due to closure of lagoon mouth, the lagoon become stock pollutant, consequently the population of foraminiferal species was minimal. The sampling stations from the beach environment (TP-1, TP-2, TP-3 and TP-4) showed lower values of heavy metal concentrations and it causes the increase of the absolute abundance of foraminiferal assemblages. During pre-monsoon, the lagoon mouth has been opened by the natural (waves and currents) and anthropogenic forces. Due to inflow and outflow of water the concentrations of the studied heavy metals were decreased and it causes the rapid increase of foraminiferal abundance in the lagoon. The AEI shows the higher value from the lagoon during monsoon and it has decreased during pre-monsoon. FI showed <2 in both the seasons. This may be due to anthropogenic influx including heavy metal pollution, nutrient pollution, agricultural runoff, domestic and industrial effluents. FI indicates environmental conditions that support substantial population of stress tolerant taxa. Factors analysis shows the distinct information about heavy metals distribution and set cluster of similar factor (Fe, Cu, Cd, Zn and Cr) during both the seasons of the study under investigation.

6. Conclusions

- The heavy metals and benthic foraminiferal distribution infer that the Tupilipalem coast is ecologically stressed owing to lagoon mouth dynamics.
- The strong northern wind triggers an oblique wave approach to the shoreline, resulting the closing of the lagoon mouth.

- The heavy metals sequence as; Fe> Mn> Zn> Cr> Ni> Pb> Cu> Cd. The higher concentrations may be due to the effect of intensive anthropogenic stress as well as lagoon mouth closure in the area.
- The metal enrichment reveals that the Cd is extremely high and Pb enrichment is 70% in some stations. The PLI values of Cd is >1 during Pre-monsoon and monsoon seasons due to the influence of direct external sources like agricultural runoff and associated anthropogenic inputs.
- The Factor loadings matrix infers the heavy metal distribution and clusters of similar factors (Fe, Cu, Cd, Zn and Cr) during monsoon and pre-monsoon seasons.
- A total of 49 benthic foraminiferal species and cluster analysis results indicated that the taxonomic compositions, quantitative distributions were changed from monsoon to pre- monsoon (lagoon mouth closure to open).
- The coastal morphology and anthropogenic input as a source of heavy metals that affected the taxonomic composition and quantitative distributions of foraminiferal assemblages has been alarming.
- An AEI indicates that the hypoxic conditions from all the sampling stations except TP-12 from lagoon environment during the mouth closure. The FI values of monsoon and pre-monsoon shows <2, indicating environmental conditions that support substantial population of stress tolerant microbiota.

For the present study, the coastal morphology and anthropogenic input as a source of heavy metals and its impact on this area is affecting the taxonomic composition and quantitative distributions of foraminiferal assemblages. Moreover, this study area is considered to be the proposed site to construct a Major Sea- Port to be named as Dugarajapatnam Port soon. Therefore, sustainable development and protection of the coastal

zone is need of the hour. The periodical monitoring and migration of coastal dynamics of this area is warranted.

Ethical Approval: Not Applicable

Consent to Participate: Not Application

Consent to publish: Not Applicable

Authors Contributions:

1. *Ideas; formulation or evolution of overarching research goals, aims and development or design of methodology:* **Sreenivasulu, G.**
2. *Oversight and leadership responsibility for the research activity planning and execution, including mentorship external to the core team:* **Jayaraju, N., Reddy, A.N.**
3. *Provision of study materials, materials, laboratory, instrumentation, computing resources, or other analysis tools:* **Prakash, T.N., Nagendra, R., Sheela Nair, L.**
4. *Application of statistical, mathematical, computational, or other formal techniques to analyze or synthesize study data:* **Lakshmana, B., Tiju, I.V.**

Funding : This work was supported by Department of Science and Technology (DST), Govt. of India in the form of DST-INSPIRE Fellowship (No. DST/INSPIRE Fellowship/2012/344-IF120311).

Competing Interests: The authors of this manuscript declare that there are no competing interests.

Availability of Data and Materials: Most data generated or analyzed during this study are included in this manuscript. Further data used during the current study are available from the corresponding author on reasonable request.

Acknowledgements

G. Sreenivasulu is thankful to the DST, New Delhi, India for the financial support in the form of DST-INSPIRE Fellowship (No. DST/INSPIRE Fellowship/2012/344- IF120311).

References

- Adarsh, P., Rajeshwara Rao, N., 2012. Benthic foraminifera from onshore trench samples at Vengara and Punchakkad, Kannur district, Kerala: Implications for sea-level changes. *International Journal of Earth Sciences and Engineering*, 5(4), 731–738.
- Ahmed, F., Fakhruddin, A. N. M., Imam, M. D. T., Khan, N., Khan, T. A., Rahman, M. M., Abdullah, A. T. M., 2016. Spatial distribution and source identification of heavy metal pollution in roadside surface soil: a study of Dhaka Aricha highway, Bangladesh. *Ecological Processes*, 5(1), 2. <https://doi.org/10.1186/s13717-016-0045-5>
- Ansari, T. M., Marr, I. L., Tariq, N., 2003. Heavy Metals in Marine Pollution Perspective—A Mini Review. *Journal of Applied Sciences*, 4(1), 1–20. <https://doi.org/10.3923/jas.2004.1.20>
- Boltovskoy, E., Scott, D., Medioli, F., 2021. Morphological Variations of Benthic Foraminiferal Tests in Response to Changes in Ecological Parameters: A Review on JSTOR. *Journal of Paleontology*, , 65(2), 175–185. <http://www.jstor.org/stable/1305752>
- Bouchet, V. M. P., Alve, E., Rygg, B., Telford, R. J., 2012. Benthic foraminifera provide a promising tool for ecological quality assessment of marine waters. *Ecological Indicators*, 23(2012), 66–75. <https://doi.org/10.1016/j.ecolind.2012.03.011>
- Bouchet, V. M. P., Deldicq, N., Baux, N., Dauvin, J. C., Pezy, J. P., Seuront, L., Méar, Y., 2020. Benthic foraminifera to assess ecological quality statuses: The case of salmon fish farming. *Ecological Indicators*, 117, 106607. <https://doi.org/10.1016/j.ecolind.2020.106607>
- Cardoso, S. J., Quadra, G. R., Resende, N. da S., Roland, F., 2019. The role of sediments in

- the carbon and pollutant cycles in aquatic ecosystems. *Acta Limnologica Brasiliensia*, 31, 201. <https://doi.org/10.1590/s2179-975x8918>
- Carnahan, E. A., Hoare, A. M., Hallock, P., Lidz, B. H., Reich, C. D., 2009. Foraminiferal assemblages in Biscayne Bay, Florida, USA: Responses to urban and agricultural influence in a subtropical estuary. *Marine Pollution Bulletin*, 59(8–12), 221–233. <https://doi.org/10.1016/j.marpolbul.2009.08.008>
- Chenthamilselvan, S., Kankara, R. S., Rajan, B., 2014. Assessment of shoreline changes along Karnataka coast, India using GIS & Remote sensing techniques. In *Indian Journal of Geo-Marine Sciences*, 43(7). <http://nopr.niscair.res.in/handle/123456789/34441>
- Cochard, R., 2017. Coastal Water Pollution and its Potential Mitigation by Vegetated Wetlands: An Overview of Issues in Southeast Asia. In *Redefining Diversity and Dynamics of Natural Resources Management in Asia*, 1, 189–230). Elsevier Inc. <https://doi.org/10.1016/B978-0-12-805454-3.00012-8>
- Crain, C. M., Halpern, B. S., Beck, M. W., Kappel, C. V., 2009. Understanding and managing human threats to the coastal marine environment. In *Annals of the New York Academy of Sciences*, 1162(1), 39–62. Blackwell Publishing Inc. <https://doi.org/10.1111/j.1749-6632.2009.04496.x>
- Foraminifera Gallery-illustrated catalog www.foraminifera.eu.
- Ganugapenta, S., Nadimikeri, J., Chinnapolla, S. R. R. B., Ballari, L., Madiga, R., K, N., Tella, L. P., 2018. Assessment of heavy metal pollution from the sediment of Tupilipalem Coast, southeast coast of India. *International Journal of Sediment Research*. <https://doi.org/10.1016/j.ijsrc.2018.02.004>
- Gesamp, 1985. Un/fao/unesco/who/wmo/iaea/unep Joint Group of Experts on the Scientific Aspects of Marine Pollution: Cadmium, lead and tin in the marine environment. Reports and Studies No. 26.

- Gheorghe, S., Stoica, C., Vasile, G. G., Nita-Lazar, M., Stanescu, E., Lucaciu, I. E., 2017. Metals Toxic Effects in Aquatic Ecosystems: Modulators of Water Quality. In Water Quality. InTech. <https://doi.org/10.5772/65744>
- He, M., Hu, B., Chen, B., Jiang, Z., 2017. Inductively coupled plasma optical emission spectrometry for rare earth elements analysis. *Physical Sciences Reviews*, 2(1). <https://doi.org/10.1515/psr-2016-0059>
- Henry B. Brady., 1884. Report on the Foraminifera Dredged by H.M.S. ‘Challenger’ During the Years 1873–1876. — Rept. Sei. Results Explor. Voyage H.M.S., 49. ‘Challenger’, Zoology. <http://www.19thcenturyscience.org/HMSC/HMSC-Reports/Zool-22/htm/doc.html>
- Holzhauser, H., Borsje, B. W., van Dalssen, J. A., Wijnberg, K. M., Hulscher, S. J. M. H., Herman, P. M. J., 2020. Benthic species distribution linked to morphological features of a barred coast. *Journal of Marine Science and Engineering*, 8(1). <https://doi.org/10.3390/JMSE8010016>
- Izzati Minhat, F., Yahya, K., Talib, A., Ahmad, O., 2013. A survey of benthic assemblages of Foraminifera in tropical coastal waters of Pulau Pinang, Malaysia. *Tropical Life Sciences Research*, 24(1), 35–43. </pmc/articles/PMC3799408/>
- Jayaraju, N., Sundara, B. C., Reddy, R., Reddy, K. R., 2010. Impact of Dredging on Sediment of Krishnapatnam Port, East Coast of India: Implications for Marine Biodiversity. In *Journal of Environmental Science and Engineering* 4(8), 66-75.
- Kowalska, J. B., Mazurek, R., Gąsiorek, M., Zaleski, T., 2018. Pollution indices as useful tools for the comprehensive evaluation of the degree of soil contamination—A review. In *Environmental Geochemistry and Health*, 40(6), 2395–2420). Springer Netherlands. <https://doi.org/10.1007/s10653-018-0106-z>
- Lai, C. T., Gardner, H., Geddes, D., 2018. Comparison of inductively coupled plasma optical

- emission spectrometry with an ion selective electrode to determine sodium and potassium levels in human milk. *Nutrients*, 10(9). <https://doi.org/10.3390/nu10091218>
- Liu, P., Hu, W., Tian, K., Huang, B., Zhao, Y., Wang, X., Zhou, Y., Shi, B., Kwon, B. O., Choi, K., Ryu, J., Chen, Y., Wang, T., Khim, J. S., 2020. Accumulation and ecological risk of heavy metals in soils along the coastal areas of the Bohai Sea and the Yellow Sea: A comparative study of China and South Korea. *Environment International*, 137, 105519. <https://doi.org/10.1016/j.envint.2020.105519>
- Loeblich, A.R., Tappan, H., 1987. Foraminiferal Genera and Their Classification. Van Nostrand Reinhold (970, 847).
- Martins, M. V. A., Pinto, A. F. S., Frontalini, F., da Fonseca, M. C. M., Terroso, D. L., Laut, L. L. M., Zaaboub, N., da Conceição Rodrigues, M. A., Rocha, F., 2016. Can benthic foraminifera be used as bio-indicators of pollution in areas with a wide range of physicochemical variability? *Estuarine, Coastal and Shelf Science*, 182, 211–225. <https://doi.org/10.1016/j.ecss.2016.10.011>
- Muhammad, N.S., Fadzil, M.A., Kok, P.H., Rabitah, N.D., 2020. Upwelling in the northwest Sabah during the northeast monsoon and its relation with El-Niño. *Research in Marine Sciences*, 5(2), 681–698.
- Muller, G., 1969. Index of Geoaccumulation in Sediments of the Rhine River. *Journal of Geology*, 2, 108-118.
- Pandey, J., Singh, R., 2017. Heavy metals in sediments of Ganga River: up- and downstream urban influences. *Applied Water Science*, 7(4), 1669–1678. <https://doi.org/10.1007/s13201-015-0334-7>
- Paleontologia Electronica Webmaster 1998–2015.
- Pati, P., Patra, P. K., 2012. Benthic Foraminiferal Responses To Coastal Pollution : *International Journal Geology Earth Environmental Sciences*, 2(1), 42–56.

- Praveena, M.S., Radojevic, M., Abdullah, M.H., 2007. The assessment of man- grove sediment quality in Mengkabong Lagoon: An index analysis approach. *International Journal of Environmental Science Education*, 2(3), 60–68.
- Qian, Y., Zhang, W., Yu, L., Feng, H., 2015. Metal Pollution in Coastal Sediments. In *Current Pollution Reports*, 1(4), 203–219. Springer. <https://doi.org/10.1007/s40726-015-0018-9>
- Reid, A. J., Carlson, A. K., Creed, I. F., Eliason, E. J., Gell, P. A., Johnson, P. T. J., Kidd, K. A., MacCormack, T. J., Olden, J. D., Ormerod, S. J., Smol, J. P., Taylor, W. W., Tockner, K., Vermaire, J. C., Dudgeon, D., Cooke, S. J., 2019. Emerging threats and persistent conservation challenges for freshwater biodiversity. *Biological Reviews*, 94(3), 849–873. <https://doi.org/10.1111/brv.12480>
- Roff, J. C., Taylor, M. E., Laughren, J., 2003. Geophysical approaches to the classification, delineation and monitoring of marine habitats and their communities. In *Aquatic Conservation: Marine and Freshwater Ecosystems*, 13(1), 77–90. <https://doi.org/10.1002/aqc.525>
- Sen Gupta, B. K., Platon, E., 2006. Tracking Past Sedimentary Records of Oxygen Depletion in Coastal Waters: Use of the Ammonia-Elphidium Foraminiferal Index. In *Source: Journal of Coastal Research: III*. <https://www.jstor.org/stable/25742974?seq=1&cid=pdf->
- Shirani, M., Afzali, K. N., Jahan, S., Strezov, V., Soleimani-Sardo, M., 2020. Pollution and contamination assessment of heavy metals in the sediments of Jazmurian playa in southeast Iran. *Scientific Reports*, 10(1), 1–11. <https://doi.org/10.1038/s41598-020-61838-x>
- Short, A. D., Jackson, D. W. T., 2013. Beach Morphodynamics. In *Treatise on Geomorphology*, 10, 106–129. Elsevier Inc. <https://doi.org/10.1016/B978-0-12-374739->

6.00275-X

- Singh, R., Gautam, N., Mishra, A., Gupta, R., 2011. Heavy metals and living systems: An overview. In *Indian Journal of Pharmacology*, 43(3), 246–253. Wolters Kluwer -- Medknow Publications. <https://doi.org/10.4103/0253-7613.81505>
- Solai, A., Gandhi, M. S., Rao, N. R., 2013. Recent benthic foraminifera and their distribution between Tuticorin and Tiruchendur, Gulf of Mannar, south-east coast of India. *Arabian Journal of Geosciences*, 6(7), 2409–2417. <https://doi.org/10.1007/s12517-011-0514-1>
- Soliman, N. F., Nasr, S. M., Okbah, M. A., 2015. Potential ecological risk of heavy metals in sediments from the Mediterranean coast, Egypt. *Journal of Environmental Health Science and Engineering*, 13(1), 1–12. <https://doi.org/10.1186/s40201-015-0223-x>
- Sreenivasulu, G., Jayaraju, N., Sundara, B. C., Reddy, R., Lakshmana, B., Prasad, T. L., 2018. Influence of coastal morphology on the distribution of heavy metals in the coastal waters of Tupilipalem coast, Southeast coast of India. *Remote Sensing Applications: Society and Environment*, 10, 190–197. <https://doi.org/10.1016/j.rsase.2018.04.003>
- Sreenivasulu, G., Jayaraju, N., Sundara Raja Reddy, B. C., Lakshmi Prasad, T., Lakshmana, B., Nagalakshmi, K., 2017. Coastal morphodynamics of Tupilipalem Coast, Andhra Pradesh, southeast coast of India. *Current Science*, 112(4), 823–829. <https://doi.org/10.18520/cs/v112/i04/823-829>
- Sreenivasulu, G., Jayaraju, N., Sundara Raja Reddy, B. C., Lakshmi Prasad, T., Lakshmana, B., Nagalakshmi, K., Prashanth, M., 2016. River mouth dynamics of Swarnamukhi estuary, Nellore coast, southeast coast of India. *Geodesy and Geodynamics*, 7(6), 387–395. <https://doi.org/10.1016/j.geog.2016.09.003>
- Sreenivasulu, G., Jayaraju, N., Sundara Raja Reddy, B. C., Lakshmi Prasad, T., Nagalakshmi, K., Lakshmana, B., 2017a. Foraminiferal research in coastal ecosystems of India during the past decade: A review. *GeoResJ*, 13, 38–48.

<https://doi.org/10.1016/j.grj.2017.02.003>

- Sreenivasulu, G., Jayaraju, N., Sundara Raja Reddy, B. C., Lakshmi Prasad, T., Nagalakshmi, K., Lakshmana, B., 2017b. Organic matter from benthic foraminifera (*Ammonia beccarii*) shells by FT-IR spectroscopy: A study on Tupilipalem, South east coast of India. *MethodsX*, 4, 55–62. <https://doi.org/10.1016/j.mex.2017.01.001>
- Sreenivasulu, G., Praseetha, B. S., Daud, N. R., Varghese, T. I., Prakash, T. N., Jayaraju, N. 2019. Benthic foraminifera as potential ecological proxies for environmental monitoring in coastal regions: A study on the Beypore estuary, Southwest coast of India. *Marine Pollution Bulletin*. <https://doi.org/10.1016/j.marpolbul.2018.11.058>
- Suresh Gandhi, M., Jisha, K., 2017. Foraminiferal and sediment geochemistry studies in and around Cochin backwaters, southwest coast of India. In *Indian Journal of Geo Marine Sciences*, 46(11).
- Sutherland, R. A., 2000. Bed sediment-associated trace metals in an urban stream, Oahu, Hawaii. *Environmental Geology*, 39(6), 611–627. <https://doi.org/10.1007/s002540050473>
- Tian, K., Wu, Q., Liu, P., Hu, W., Huang, B., Shi, B., Zhou, Y., Kwon, B. O., Choi, K., Ryu, J., Seong Khim, J., Wang, T., 2020. Ecological risk assessment of heavy metals in sediments and water from the coastal areas of the Bohai Sea and the Yellow Sea. *Environment International*, 136, 105512. <https://doi.org/10.1016/j.envint.2020.105512>
- Trevizan, L. C., Nóbrega, J. A., 2007. Inductively coupled plasma optical emission spectrometry with axially viewed configuration: An overview of applications. In *Journal of the Brazilian Chemical Society*, 18(4), 678–690. Sociedade Brasileira de Quimica. <https://doi.org/10.1590/S0103-50532007000400003>
- Varol, M., 2011. Assessment of heavy metal contamination in sediments of the Tigris River (Turkey) using pollution indices and multivariate statistical techniques. *Journal of*

Hazardous Materials, 195, 355–364. <https://doi.org/10.1016/j.jhazmat.2011.08.051>

Virginia Alves Martins, M., Yamashita, C., Helena de Mello e Sousa, S., Apostolos Machado

Koutsoukos, E., Trevisan Disaró, S., Debenay, J.-P., Duleba, W., 2019. Response of Benthic Foraminifera to Environmental Variability: Importance of Benthic Foraminifera in Monitoring Studies. In Monitoring of Marine Pollution. IntechOpen. <https://doi.org/10.5772/intechopen.81658>

Wang, P., Sheng, J., 2016. A comparative study of wave-current interactions over the eastern Canadian shelf under severe weather conditions using a coupled wave-circulation model. Journal of Geophysical Research: Oceans, 121(7), 5252–5281. <https://doi.org/10.1002/2016JC011758>

World Modern Foraminifera Database www.marinespecies.org/foraminifera/.

Figure Captions:

Fig. 1 Location map of the study area

Fig.2 Landsat8 OLI/TIRS images showing the lagoon mouth dynamics

Fig.3 Wind direction and wind speed plots for the seven days prior to the satellite image during monsoon

Fig.4 Wind direction and wind speed plots for the seven days prior to the satellite image during pre-monsoon

Fig.5 Geoaccumulation index (I_{geo}) for the studied heavy metals.

Fig.6 Enrichment Factor (EF) for the studied heavy metals.

Fig. 7 The Pollution Load Index (PLI) for the studied heavy metals.

Fig. 8 Cross plot of Factor loadings of selected heavy metals during monsoon (a &b) and pre-monsoon. (c & d)

Fig. 9 Diversity indices of foraminifera

Fig. 10 Ecological Indices of foraminifera

Fig. 11 Significant correlation between the abundance of benthic foraminifera and sampling stations during monsoon.

Fig. 12 Significant correlation between the abundance of benthic foraminifera and sampling stations during pre-monsoon

Plate 1 -(1) *Ammonia dentata*, ventral view; (2) *A. dentata*, dorsal view (showing boring marks); (3) *A. dentata*, dorsal view; (4) *Quinqueloculina* seminulum, side view; (5) *Spiroloculina costata*, side view; (6) *Triloculina oblonga*, side view; (7) *T. oblonga*, side view; (8) *Adelosina laevigata*, side view; (9) *Asterorotalia pulchella*, ventral view; (10) *Pararotalia nipponica*, ventral view; (11) *Spiroloculina depressa*, side view; (12) *Eponides* sp.; (13) *Eponides repandes*, dorsal view; (14) *Elphidium advenum*, side view; (15) *Asterorotalia pulchella*, dorsal view; (16) *Quinqueloculina agglutinans*, side view; (17) *Elphidium jenseni*, side view; (18) *Pararotalia nipponica*, ventral view; (19) *Elphidium hispidulum*, side view; (20) *Quinqueloculina* seminulum.

Plate 2- (1) *Quinqueloculina* sp., side view; (2) *Triloculina trigonula*, side view; (3) *Discorbinella bertheloti*, ventral view; (4) *Triloculina cuneata*, side view; (5) *Quinqueloculina* sp., side view; (6) *Ammonia beccarii*, dorsal view; (7) *Triloculina fichteliana*, apertural view (boring marks seen); (8) *Asterorotalia pulchella*, dorsal view (boring marks seen); (9) *Quinqueloculina* sp, side view; (10) *Spiroloculina orbis*, side view; (11) *Elphidium discoidale*, side view; (12) *Rosalina* sp.; (13) *Hanzawaia concentrica*, ventral view; (14) *Triloculina cuneata*, side view; (15) *Elphidium craticulatum*, side view; (16) *Quinqueloculina* seminulum, side view

Table Captions:

Table 1. Heavy Metal Concentrations (ppm) from Tupilipalem coast (Monsoon).

Table 2. Heavy Metal Concentrations (ppm) from Tupilipalem coast (Premonsoon).

Table 3. Factor loadings scores for selected heavy metals.

Table 4. Distribution of benthic foraminifera from the sediments of Tupilipalem coast
(Monsoon)

Table 5. Distribution of benthic foraminifera from the sediments of Tupilipalem coast
(Premonsoon)

Table 6. Species Diversity and Ecological Indices of benthic foraminiferal assemblages.

Figures

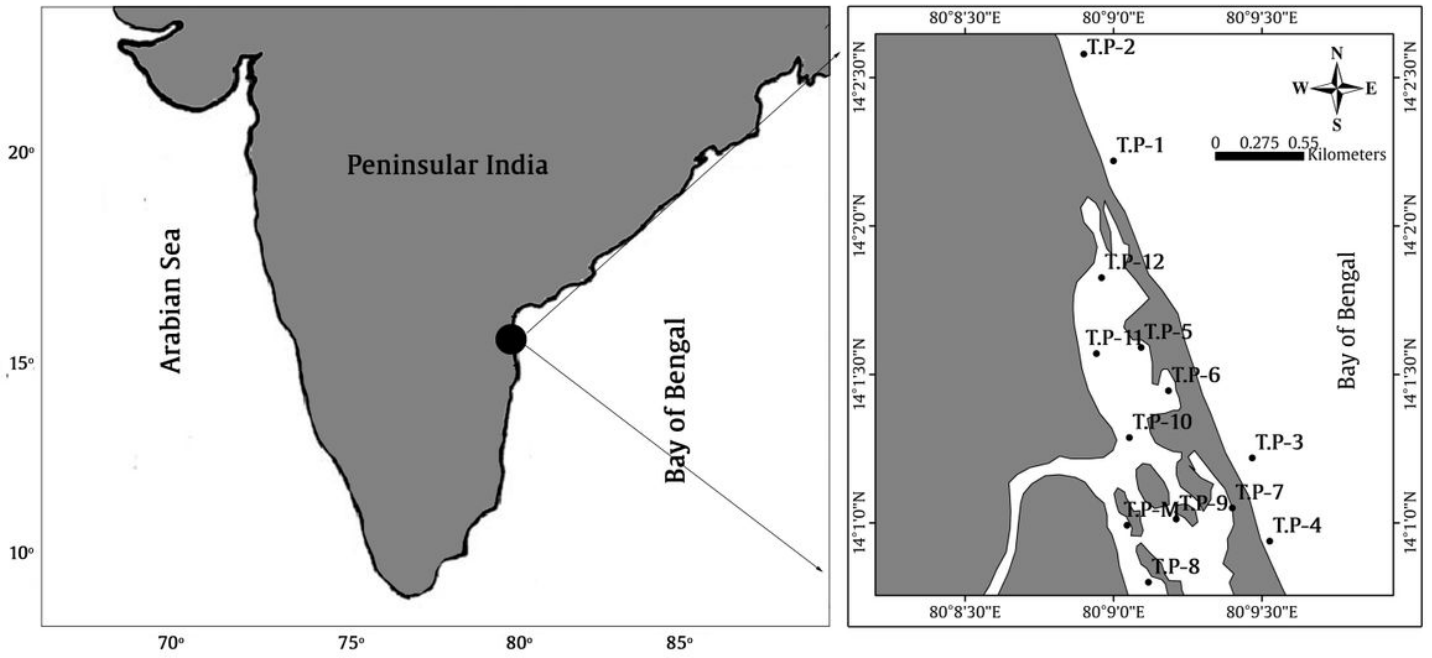


Figure 1

Location map of the study area

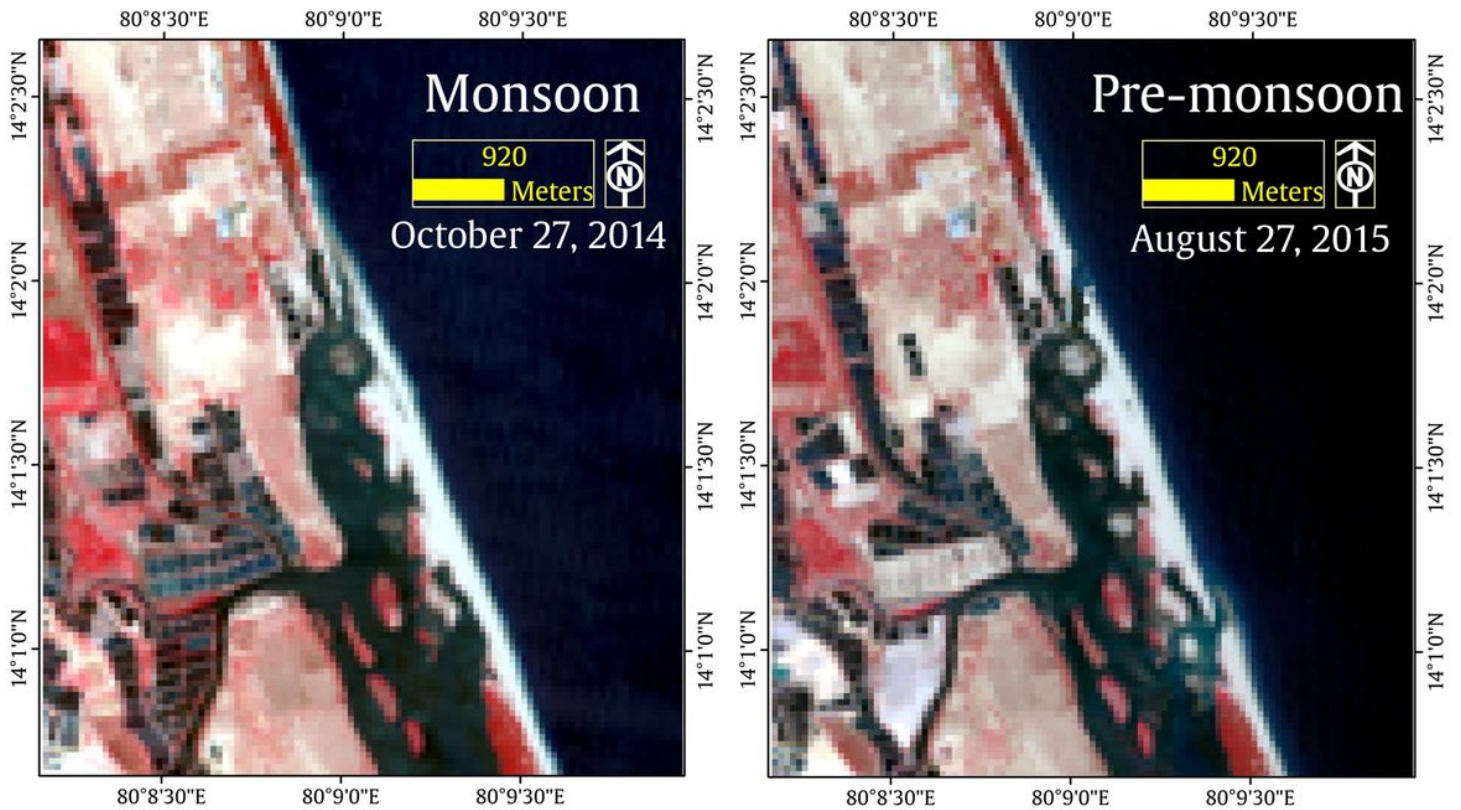


Figure 2

Landsat8 OLI/TIRS images showing the lagoon mouth dynamics

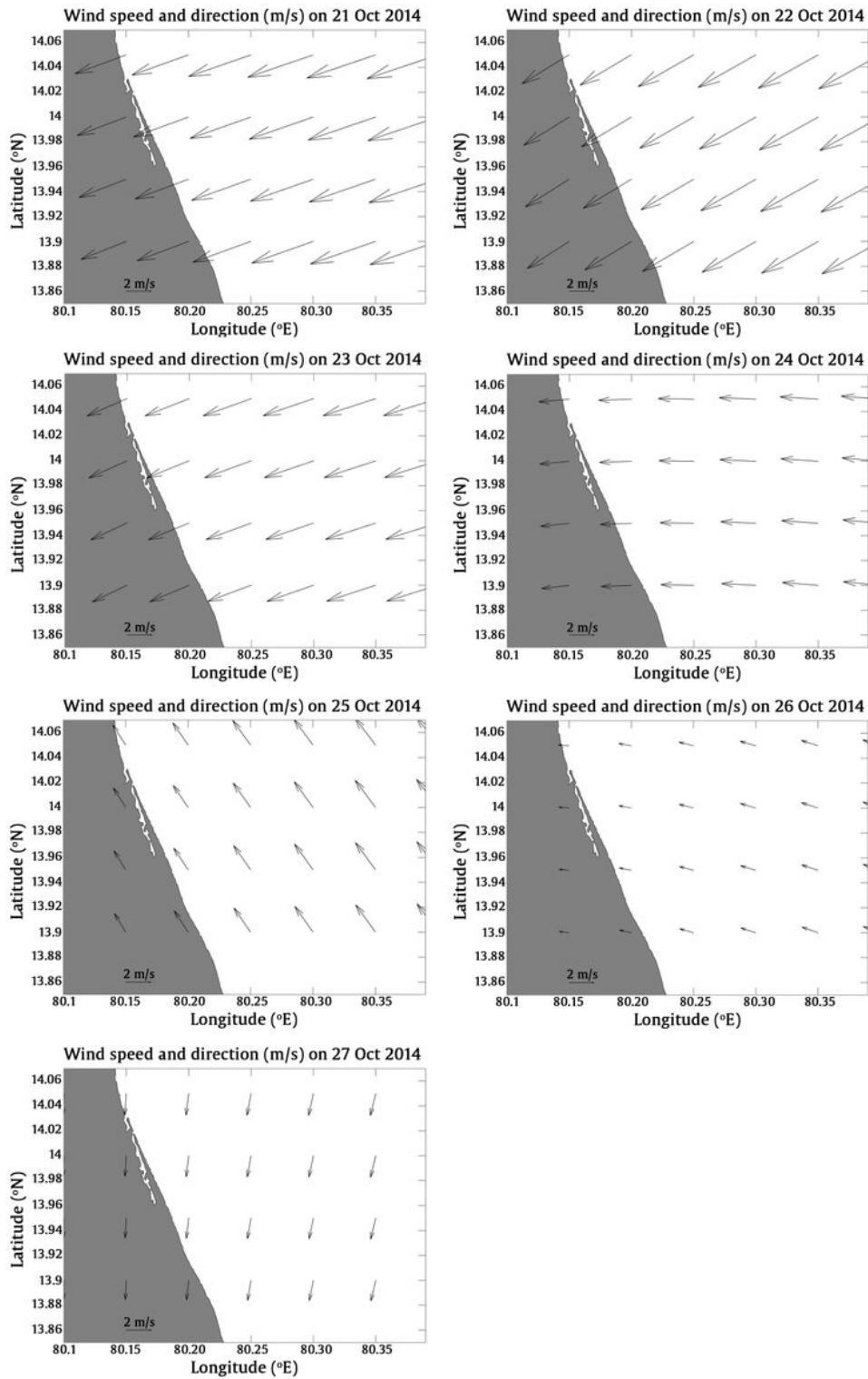


Figure 3

Wind direction and wind speed plots for the seven days prior to the satellite image during monsoon

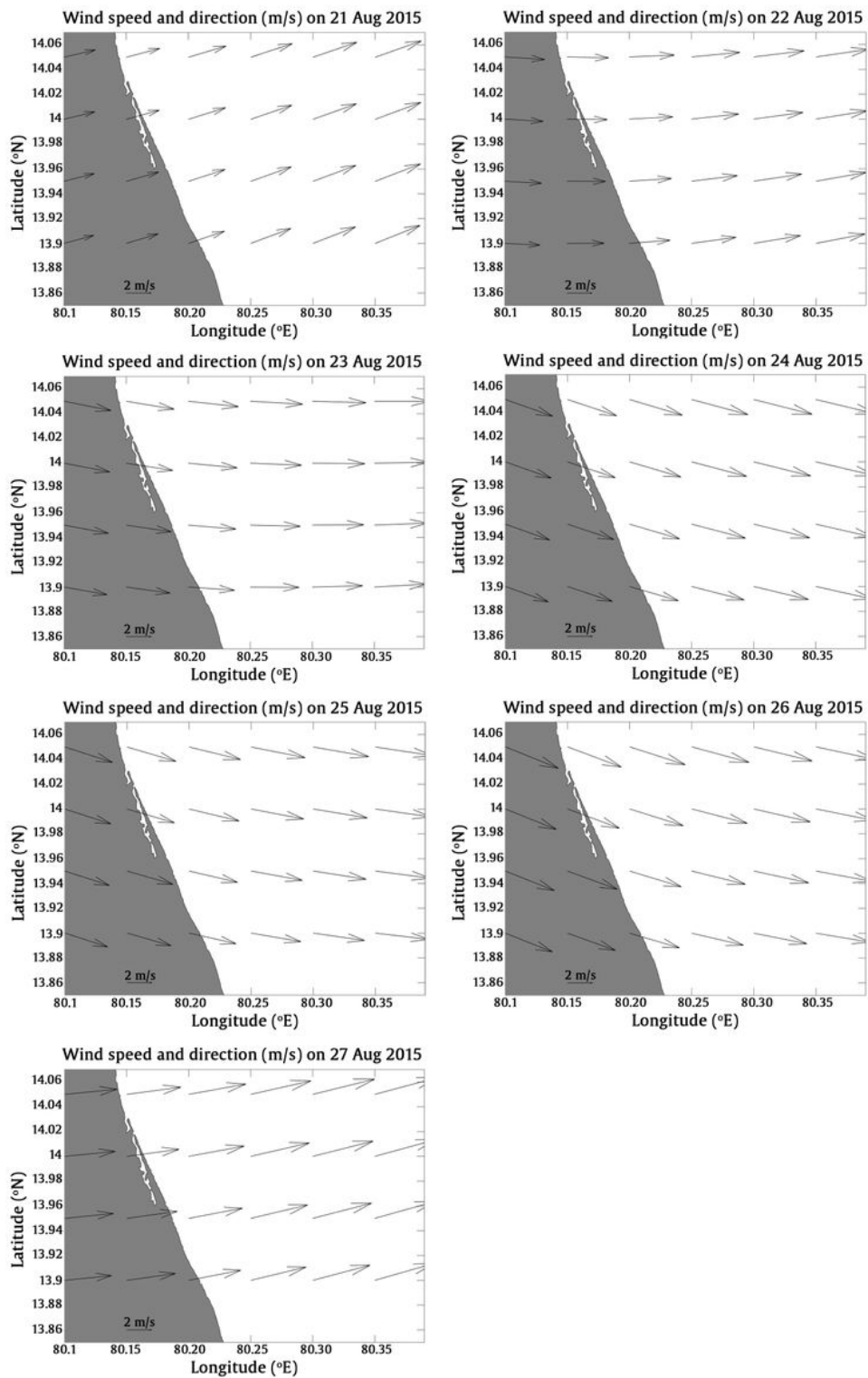


Figure 4

Wind direction and wind speed plots for the seven days prior to the satellite image during pre-monsoon

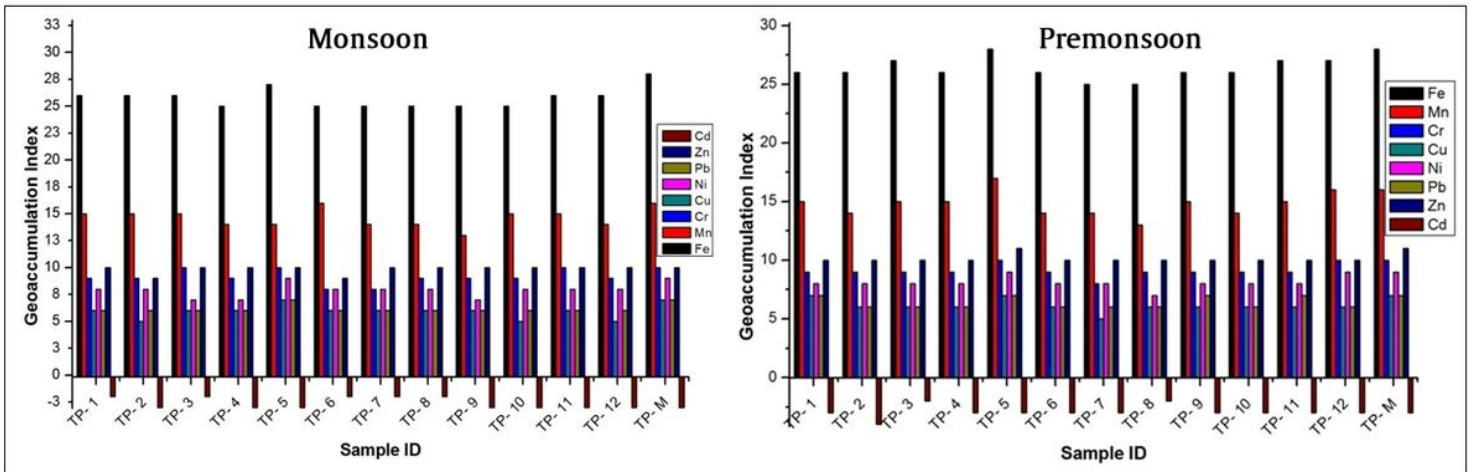


Figure 5

Geoaccumulation index (Igeo) for the studied heavy metals.

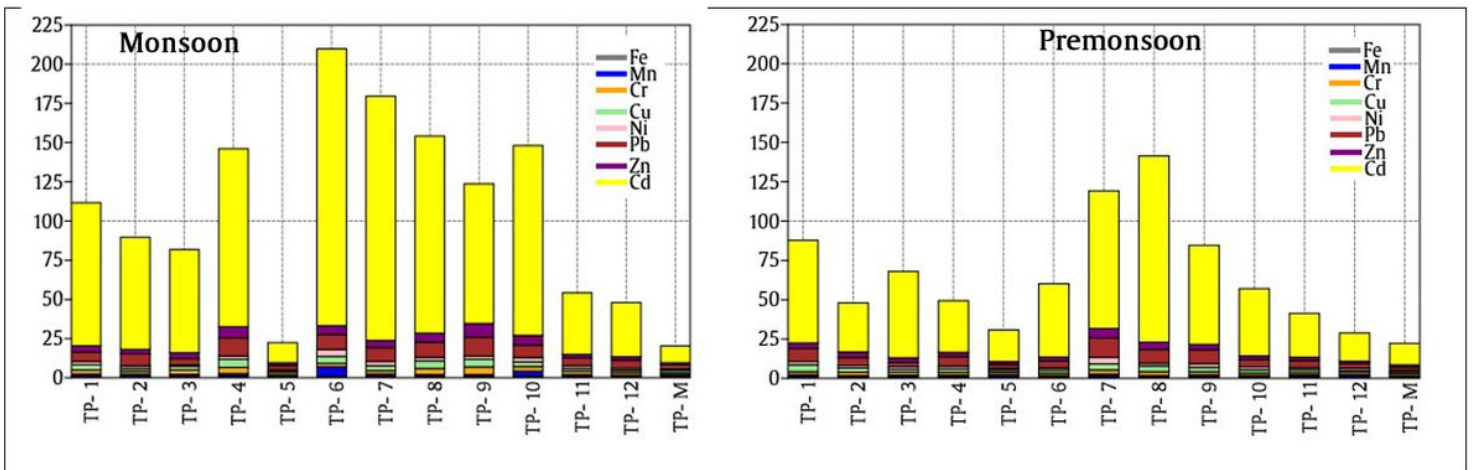


Figure 6

Enrichment Factor (EF) for the studied heavy metals.

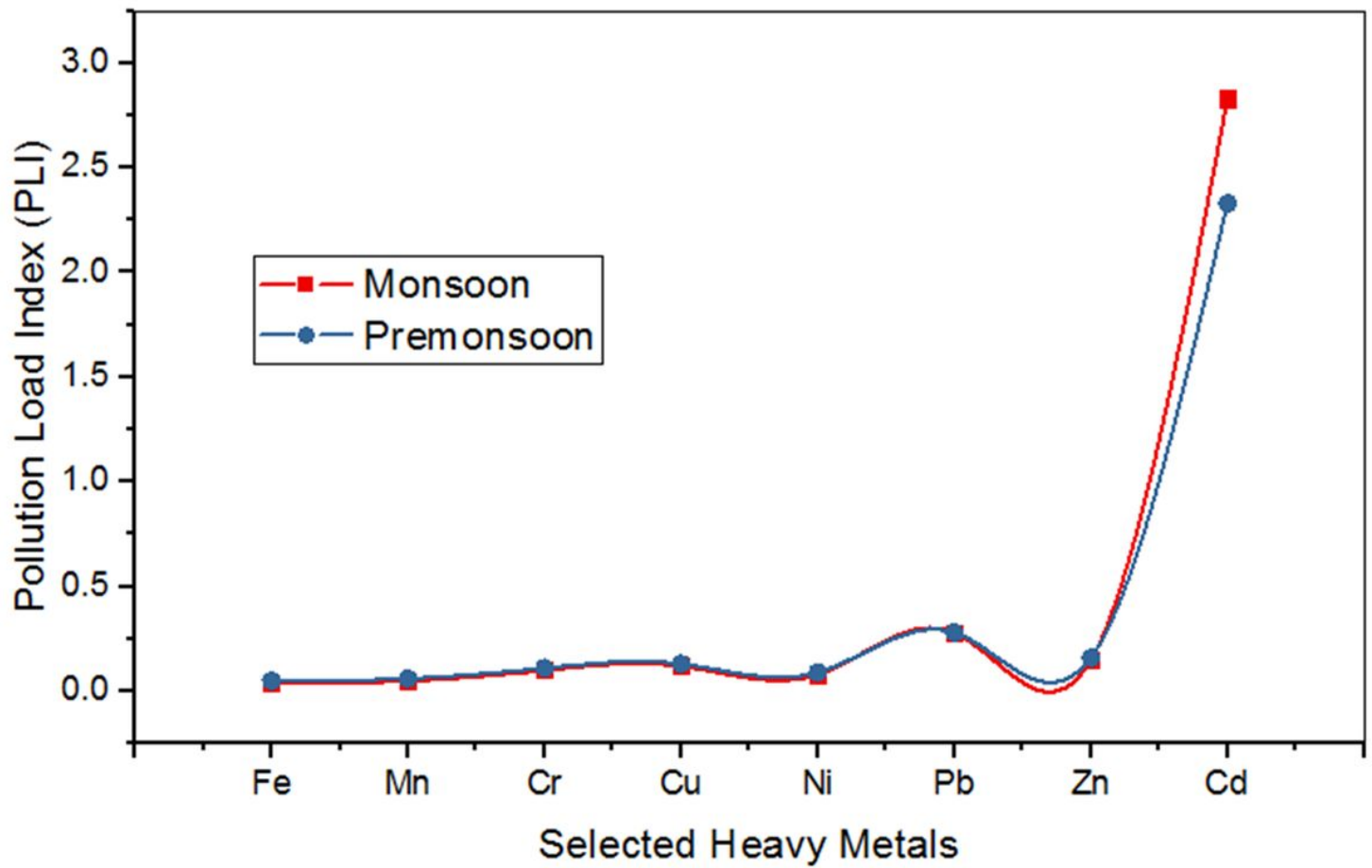


Figure 7

The Pollution Load Index (PLI) for the studied heavy metals.

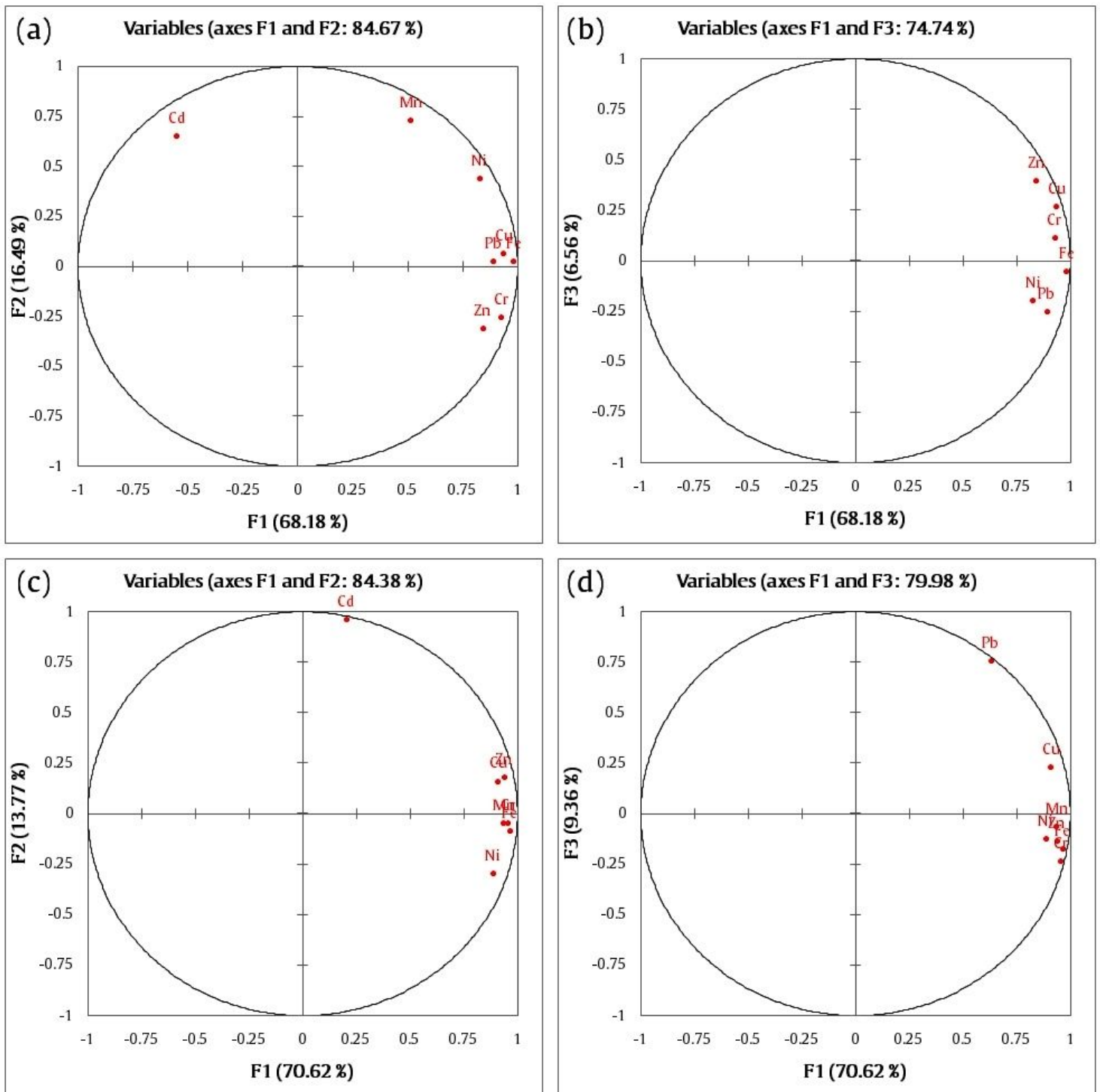


Figure 8

Cross plot of Factor loadings of selected heavy metals during monsoon (a &b) and pre- monsoon. (c & d)

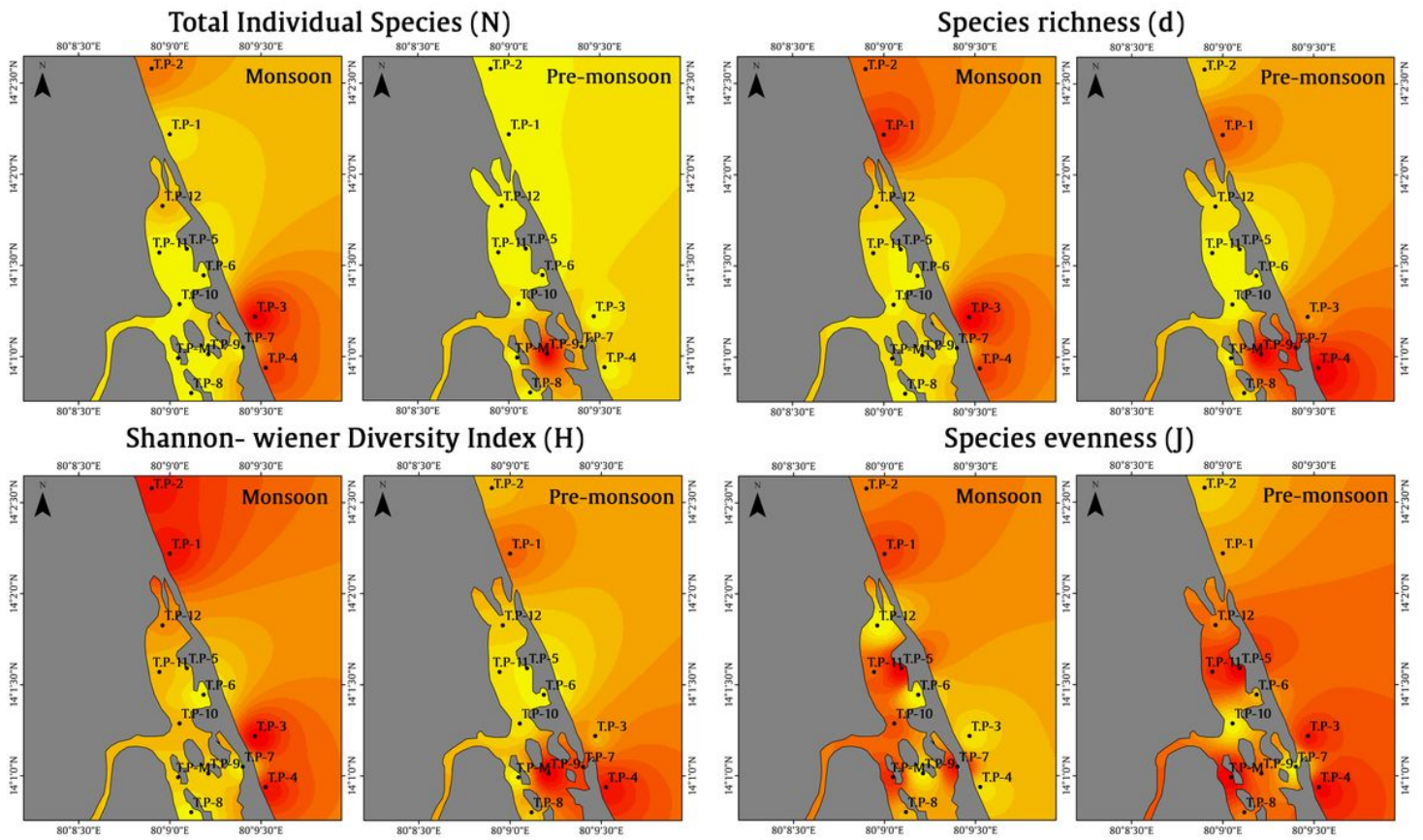
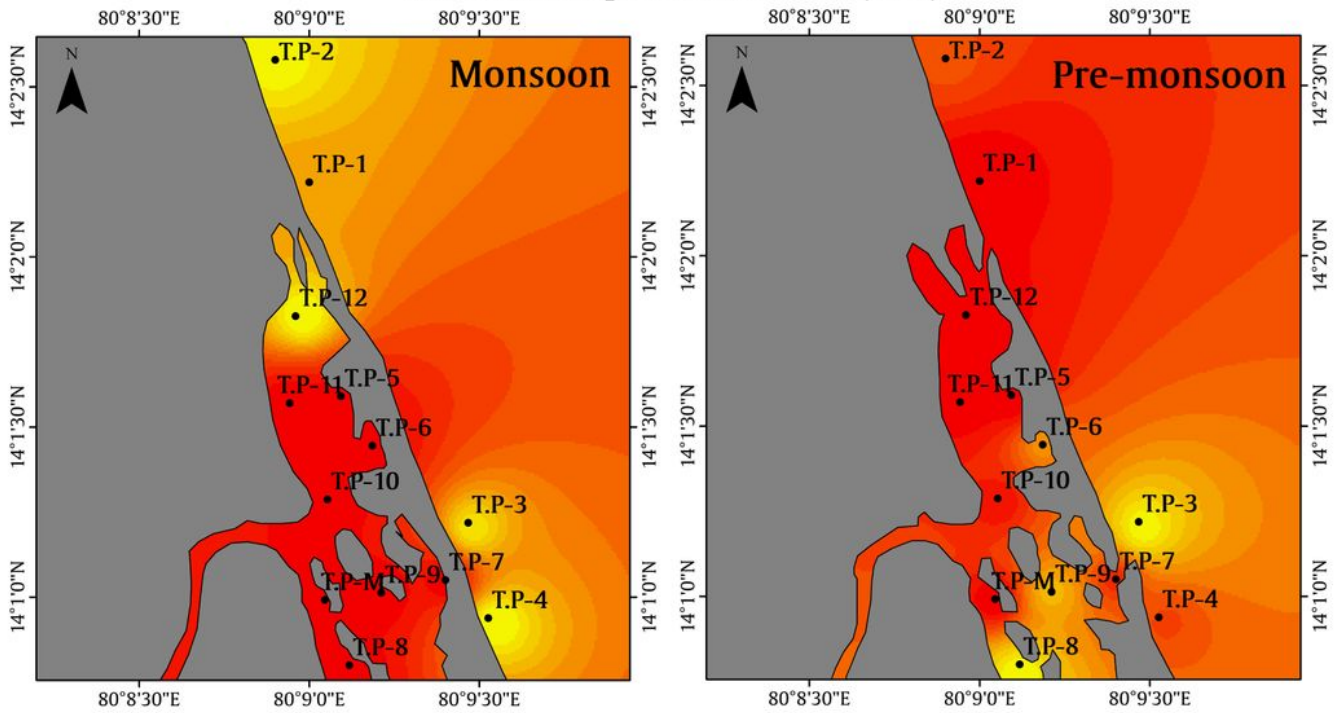


Figure 9

Diversity indices of foraminifera

Ammonia Elphidium Index (AEI)



FORAM Index (FI)

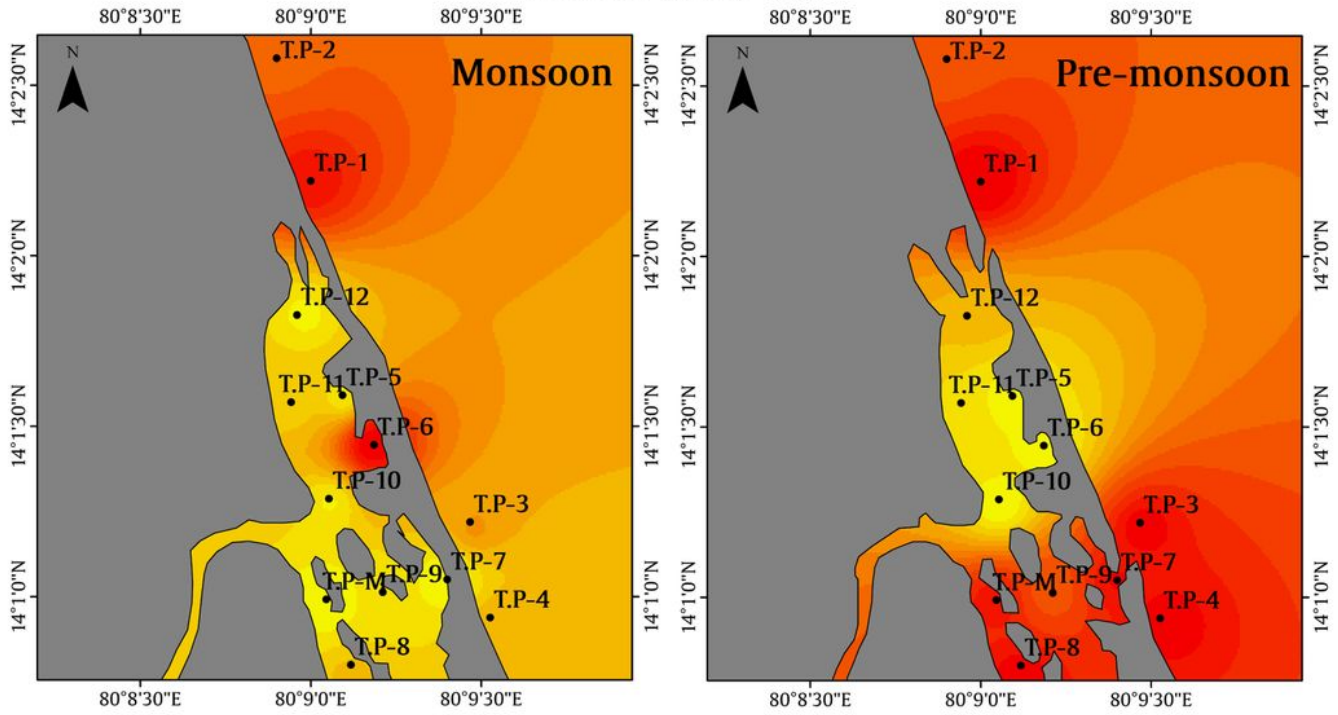


Figure 10

Ecological Indices of foraminifera

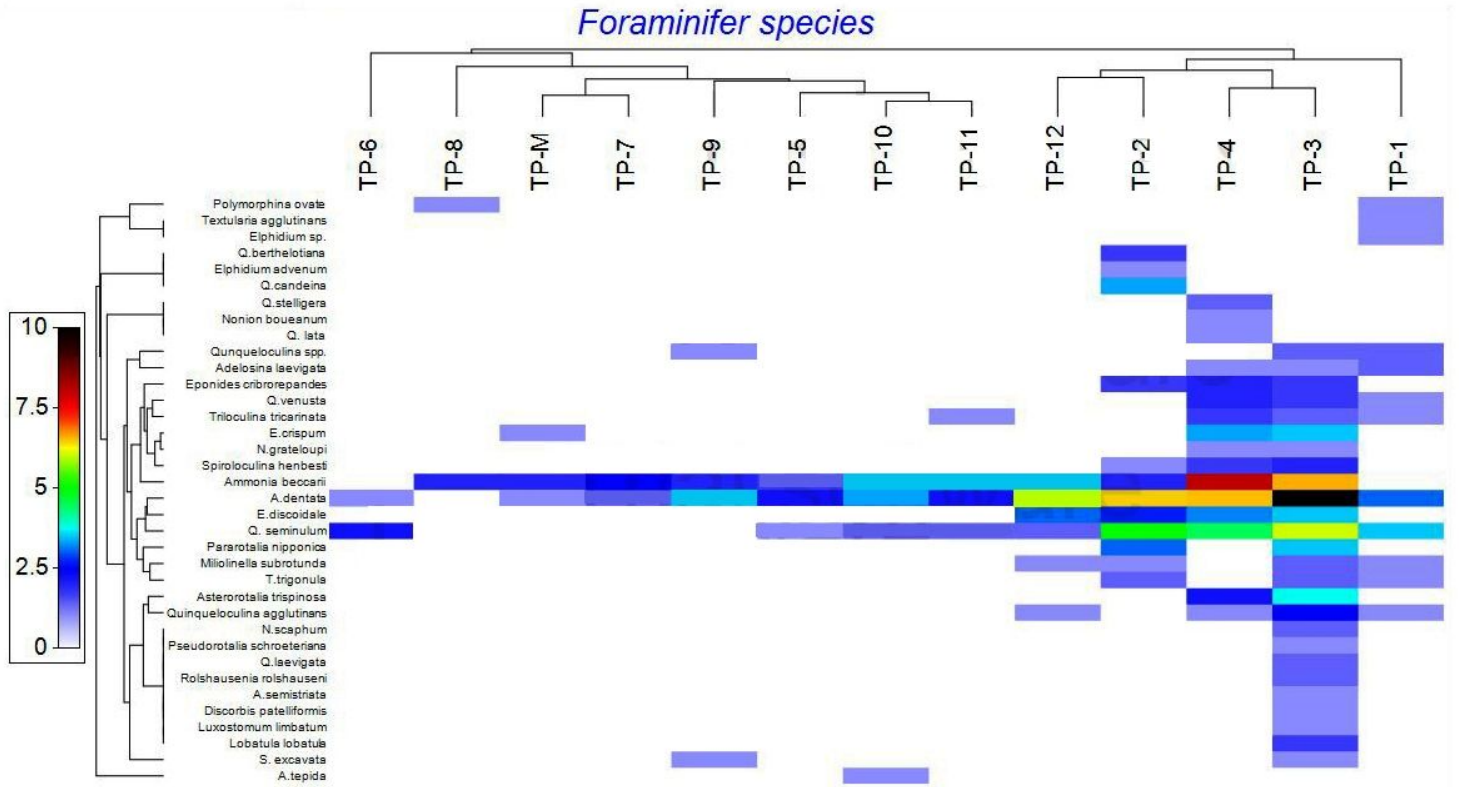


Figure 11

Significant correlation between the abundance of benthic foraminifera and sampling stations during monsoon.

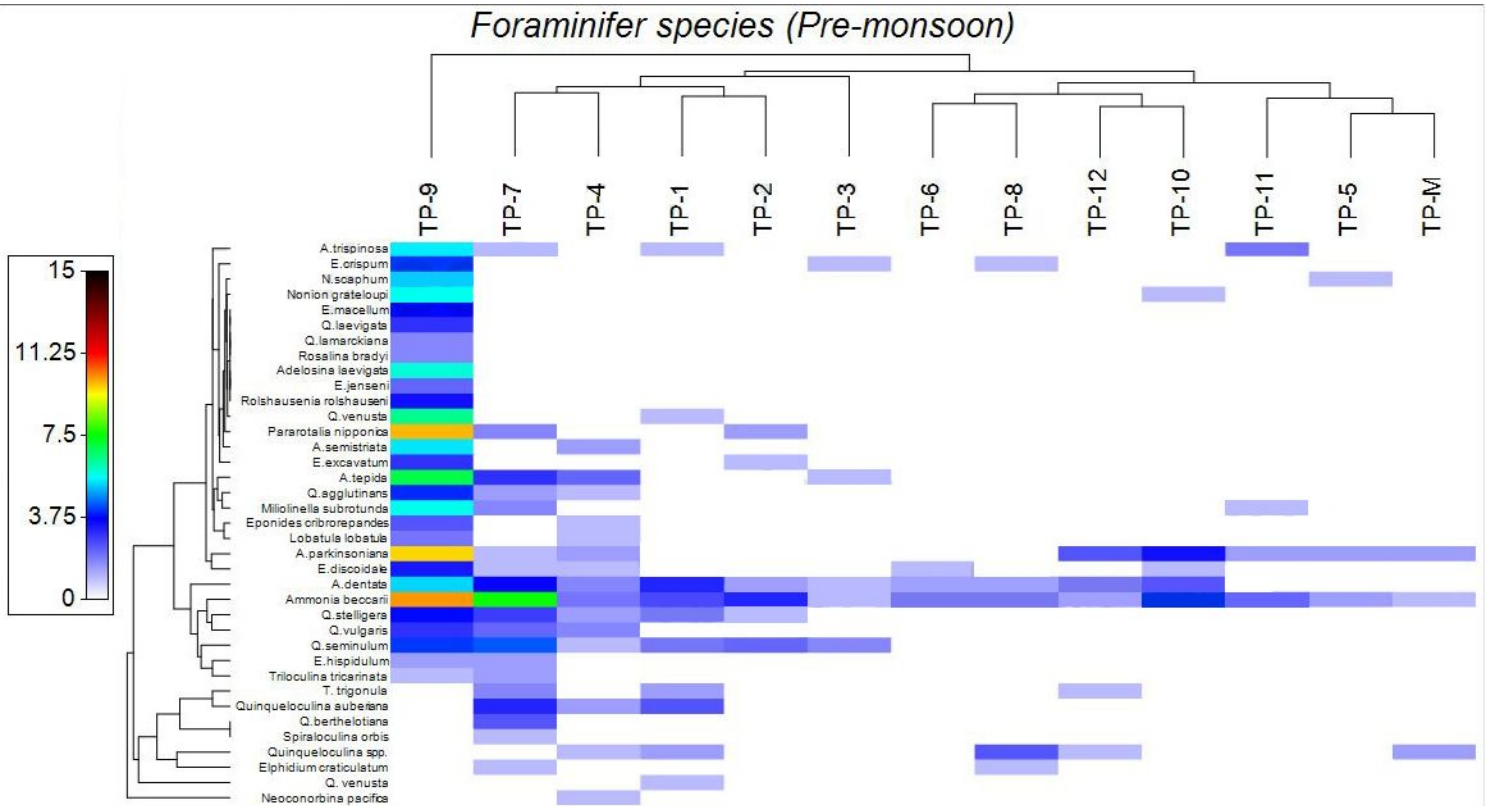


Figure 12

Significant correlation between the abundance of benthic foraminifera and sampling stations during pre-monsoon

Supplementary Files

This is a list of supplementary files associated with this preprint. Click to download.

- [PLATE1.jpg](#)
- [PLATE2.jpg](#)